Seasonality and extinction in chaotic metapopulations

B. T. GRENFELL, B. M. BOLKER† AND A. KLECZKOWSKI‡

Zoology Department, Cambridge University, Downing Street, Cambridge CB2 3EJ, U.K.

SUMMARY

A body of recent work has used coupled logistic maps to show that these model metapopulations show a decrease in global extinction rate in the chaotic region of model behaviour. In fact, many of the main ecological candidates for low-dimensional chaos are continuous-time host–parasite and predator–prey systems, driven by strong seasonal 'forcing' of one or more population parameters. This paper, therefore, explores the relation between seasonal forcing and metapopulation extinction for such systems. We base the analysis on extensive simulations of a stochastic metapopulation model for measles, based on a standard compartmental model, tracking the density of susceptible, exposed, infectious and recovered individuals (the SEIR model). The results show that, by contrast with coupled logistic maps, the increased seasonality which causes chaos maintains or increases levels of global extinction of infection, by increasing the synchrony of sub-population epidemics. The model also illustrates that the population interaction (here between susceptible and infective hosts) has a significant effect on patterns of synchrony and extinction.

1. INTRODUCTION

A recurrent theme in ecology has been the role of spatial heterogeneity in reducing the extinction rate of populations (Pimentel *et al.* 1963; Hilborn 1975; Hassell *et al.* 1991; Allen *et al.* 1993; Huffaker 1994). Recently, Allen *et al.* (1993) and Ruxton (1994) have used coupled logistic maps to derive important theoretical results about the influence of nonlinear spatial dynamics on the persistence of metapopulations. They show that increasing the average population reproductive rate (which generates the well-known transition from limit cycles to chaos in the logistic map (May 1976)) decreases local population persistence, while enhancing the overall persistence of the metapopulation. Allen *et al.* (who used stochastically perturbed maps) attribute this increase in global persistence to the effect of chaos in amplifying local noise in systems with intermediate coupling. Ruxton (1994) has since shown that this difference in local and global persistence is also generated in the deterministic case; although there is increased local extinction in the chaotic region, the fluctuations in local populations are sufficiently out of phase to reduce global extinction.

Many of the main ecological candidates for low dimensional chaos are continuous-time host–parasite and predator–prey systems, driven by strong seasonal 'forcing' of one or more population parameters (Aron & Schwartz, 1984; Olsen *et al.* 1988; Olsen & Schaffer, 1990; Hanski *et al.* 1993). In particular, there is a large quantity of literature debating the presence or absence of chaos in measles dynamics in developed countries before the vaccination era (Drepper 1988; Olsen *et al.* 1988; Pool 1989; Olsen & Schaffer 1990; Ellner 1991; Rand & Wilson 1991; Nychka *et al.* 1992). Measles is a particularly good test-bed for studies in nonlinear dynamics because of the availability both of relatively long notification time series (Fine & Clarkson 1982; Anderson *et al.* 1984; Grenfell & Anderson 1985) and plausible population models (Hamer 1906; Soper 1929; Bartlett 1957; Bartlett 1960; Black 1966; Schenzle 1984; Anderson & May 1991). Whether measles dynamics are chaotic or not, the effects of seasonality (which arises from the seasonal aggregations of children during school terms) certainly has a strong dynamical impact (Fine & Clarkson 1982; Schenzle 1984).

Viewing Allen *et al.* and Ruxton's results in the context of measles dynamics gives rise to two general questions. First, for the forced SEIR model for measles, it is increased seasonality that produces chaotic epidemic patterns (Aron & Schwartz 1984; Olsen & Schaffer 1990). However, synchronous seasonality might also be expected to magnify the correlation of subpopulations; this might then increase metapopulations extinction rates by synchronizing local extinctions. This hypothesis prompts the question: which of these roles of seasonality predominates i.e. does increasing seasonality reduce or enhance the extinction rate of model metapopulations?

The second question concerns the influence of the underlying ecological interaction on the chaos–persistence interaction. In particular, the candidates for seasonally driven chaos (notably measles and Fennoscandian vole–mustellid cycles) (Hanski *et al.* 1993) reflect the impact of seasonality on functional predator–prey interactions (represented by infectious

† Present address: Department of Ecology and Evolutionary Biology, Princeton University, Princeton, New Jersey 08544-1003, U.S.A.

‡ Present address: Department of Plant Sciences, University of Cambridge, Downing Street, Cambridge CB2 3EA, U.K.

and susceptible individuals, respectively, in the case of measles). In this broad class of systems we therefore address the question: how does the underlying population interaction affect patterns of extinction?.

In this paper we explore these issues by using simulations of a model for seasonally forced measles dynamics in a simple host metapopulation. We begin by introducing the structure of the model, then present the results of simulations, and finally discuss their ecological implications.

2. THE MODEL

(*a*) *Model structure*

We use a spatial extension of the standard compartmental model for measles: the SEIR model. Although this simple formulation has its shortcomings as a model for many aspects of measles dynamics (Schenzle 1984; Grenfell 1992; Bolker & Grenfell 1993), its well-known transition to chaos with increasing seasonal forcing of the infection rate (Aron & Schwartz 1984; Olsen & Schaffer 1990) suits our purpose here. Following Allen *et al.* (1993), we divide the constant total host population, of size into ten equal subpopulations ($N_j, j = 1, \ldots, 10$). The deterministic dynamics of infection in subpopulation j are then described by the following equations.

$$\begin{aligned} \mathrm{d}S_j/(\mathrm{d}t) &= \mu N_j - [\mu + \beta(t)\,(I_j + \Sigma_{k \neq j} v I_k)]\,S_j \\ \mathrm{d}E_j/(\mathrm{d}t) &= \beta(t)\,[I_j + v\,\Sigma_{k \neq j} I_k]\,IS - (\mu + \delta)\,E_j \\ \mathrm{d}I/(\mathrm{d}t) &= \sigma E_j - (\mu + \gamma)\,I_j. \end{aligned} \qquad (1)$$

S_j, E_j, I_j and R_j represent the density of susceptible, exposed, infectious and recovered individuals, respectively, in a constant local population of size $N_j = S_j + E_j + I_j + R_j$. Average life expectancy, disease incubation and infectious periods are $1/\mu$, $1/\sigma$ and $1/\gamma$, respectively. The infection rate of susceptibles by infectious individuals is controlled by the parameter $\beta(t)$, which is assumed to be the same for all subpopulations. Seasonality is introduced by making β an annually periodic function of time t: $\beta(t) = b_0(1 + b_1 \cos(2\pi t))$; b_1 measures the amplitude of seasonal variations around the baseline b_0. Finally, cross-infection between sites is controlled by a parameter, v, which can span the range from zero coupling ($v = 0$) to complete homogeneous mixing ($v = 1$).

(*b*) *The simulations*

Noise is introduced into the model in two ways. First, we allow for demographic noise by simulating the model with a fully stochastic Monte Carlo procedure (Bartlett 1957; Olsen *et al.* 1988; Olsen & Schaffer 1990; Bolker & Grenfell 1993). This approach allows explicitly for the probability of extinction of the infection in the troughs between epidemics. Second, we simulate environmental noise by adding multiplicative gaussian perturbations to the infection parameters (Rand & Wilson 1991).

Basic model parameters were adapted from Olsen *et al.* 1988); $b_0 = 0.010\,107$, $\sigma = 45.6$, $\gamma = 73$, $\mu = 0.02$. Unless otherwise stated, we assume a total population of $N_t = 1$ million hosts, equally divided between the

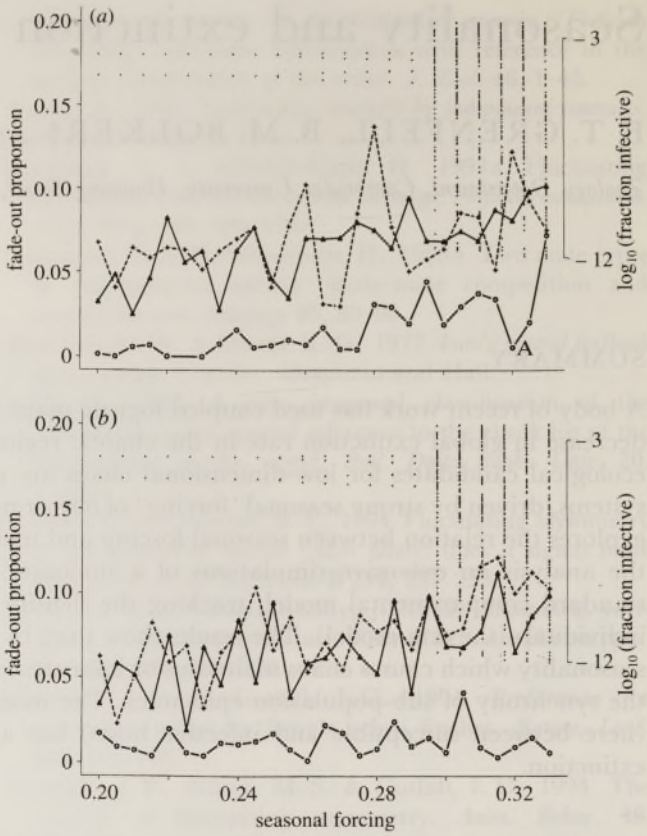

Figure 1. Level of global fadeout (extinction) of infection versus seasonal forcing amplitude for the measles metapopulation simulations described in the text. Fadeout is measured as the proportion of weeks without cases. The figure shows the results for coupling (v) equal to 0.001 (circles), 0.01 (triangles) and 0.1 (crosses), which probably spans a realistic range for developed-country urban populations (B. M. Bolker & B. T. Grenfell, unpublished results). The corresponding bifurcation diagram for the deterministic attractor is also shown on the figure (right-hand axis). At each level of seasonal forcing (b_1), the deterministic system (equations (1)) was simulated for a transient of 1000 years and then the infective density was sampled annually (at the start of each year) for 100 years to generate the points shown. (*a*) Simulations with demographic noise only. The detailed pattern of fadeout here depends partly on the structure of the attractor at each value of seasonality; for example, for $v = 0.001$ the simulations at point A ($b_1 = 0.32$) fadeout less than surrounding points. This appears to be partly due to the fact that, for many starting conditions, the deterministic attractor shows a tendency for regular (low amplitude) biennial cycles at this point in phase space; this point is taken up in the discussion. (*b*) Fadeout proportion versus seasonality for a spatial Monte Carlo model with added noise: all model parameters are as in (*a*), but now b_0 reflects 'environmental noise' – random changes affecting epidemiological processes – by incorporating 5% gaussian noise (Rand & Wilson 1991). At each Monte Carlo step, a new random variate $g(t)$ was picked from a standard normal distribution, and the effective contact rates for that step became $\{\beta(t)*[1 + 0.5*g(t)]\}$.

$m = 10$ subpopulations (which, therefore, each have population size 100 000). This metapopulation size was chosen to give significant global extinction of infection at the minimum level of seasonality used ($b_1 = 0.2$). The above level of b_0 is appropriate for an isolated population of size 100 000; for a given level of coupling (v), b_0 is scaled down by a factor of $(1 + (m-1)\,v)$, to

maintain a comparable average force of infection between simulations (Grenfell 1992). Simulation output was analysed for 100 years following a 200 year transient. A Poisson immigration rate of 21 infective individuals per year (divided equally across the model metapopulation) was used to reintroduce the infection following global extinction of the infection (Olsen *et al.* 1988; Grenfell 1992). Because these simulations are numerically very intensive we only show results for one simulation at each level of seasonality. Further numerical work (replicating a subset of simulations) indicates that the results shown below are representative of model behaviour.

3. RESULTS

(*a*) *Seasonality and fadeout*

Figure 1 shows patterns of global extinction from simulations at a range of seasonal forcing amplitudes and subpopulation couplings. Simulations with demographic noise only and demographic plus environmental noise are explored in figures 1*a*, *b*. The figures also display bifurcation diagrams (Allen *et al.* 1993), showing the transition of the deterministic SEIR model to chaotic dynamics with increasing seasonality. Overall, these results indicate that there is no tendency for decreased global fade out of infection in the chaotic region of model behaviour. Indeed, if anything, the global extinction rate increases with seasonality, particularly at the higher coupling levels ($v = 0.01, 0.1$). Because superimposing environmental noise (see figure 1*b*) onto the basic demographic variability (see figure 1*a*) does not affect this qualitative conclusion, we focus on the demographic noise case only in the rest of the analysis.

Figure 2 analyses these results in terms of the correlation structure of the metapopulation. It shows the relation between seasonality, chaos and the

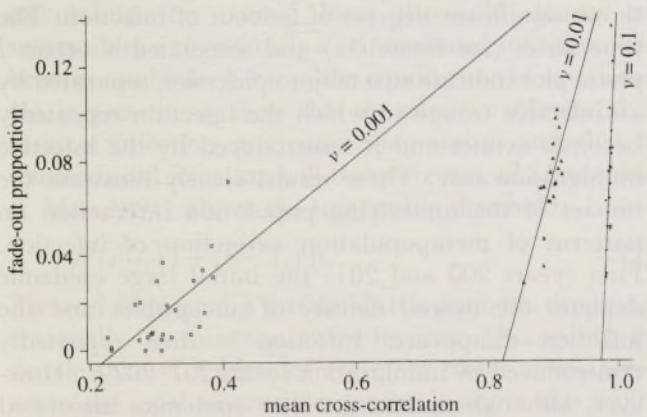

Figure 2. Cross-correlations versus fadeout proportion. The figure shows cross-correlations against fade-out proportions (weeks with zero cases) for each of the simulations shown in figure 1 (*a*). Correlations show overall means of 20 year cross-correlations (Pearson's *r*) of weekly numbers of infectives in each subpopulation. Different symbols show the range of values of cross-coupling ($v = 0.001$ (circles), 0.01 (triangles) and 0.1 (crosses). Lines are least squares regressions between fadeout (y) and correlation (x), for each level of coupling. Increased coupling between subpopulation increases average correlation (the mean position of the lines) by synchronizing large epidemics.

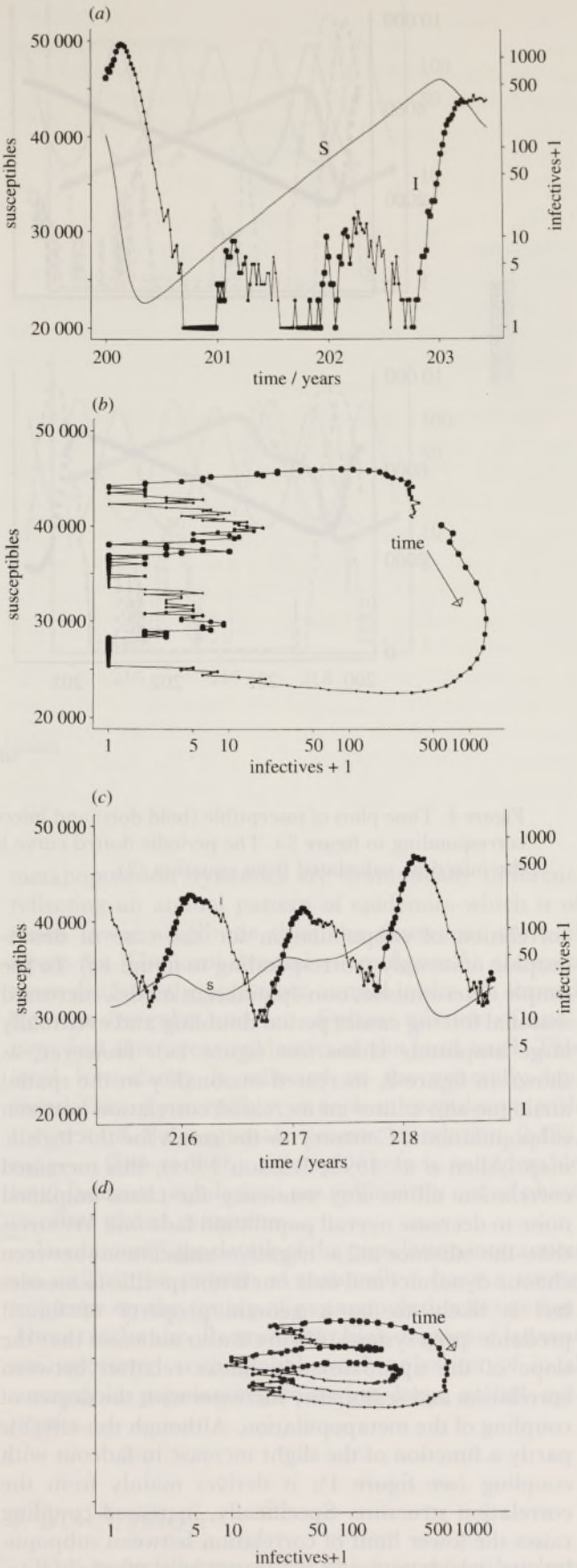

Figure 3. Dynamics of total susceptible and infective density for simulations with demographic noise only (as seen in figure 1*a*, with $b_1 = 0.33$); (*a*), (*b*) section of simulation with a period of global fadeout of infection; (*a*) and (*b*) are, respectively, time and phase space plots for susceptibles and infectives, and the dot size is proportional to the seasonal swing of infections rate ($\beta(t)$). (*c*), (*d*) As (*a*), (*b*), but for a region of the simulation with no fadeouts.

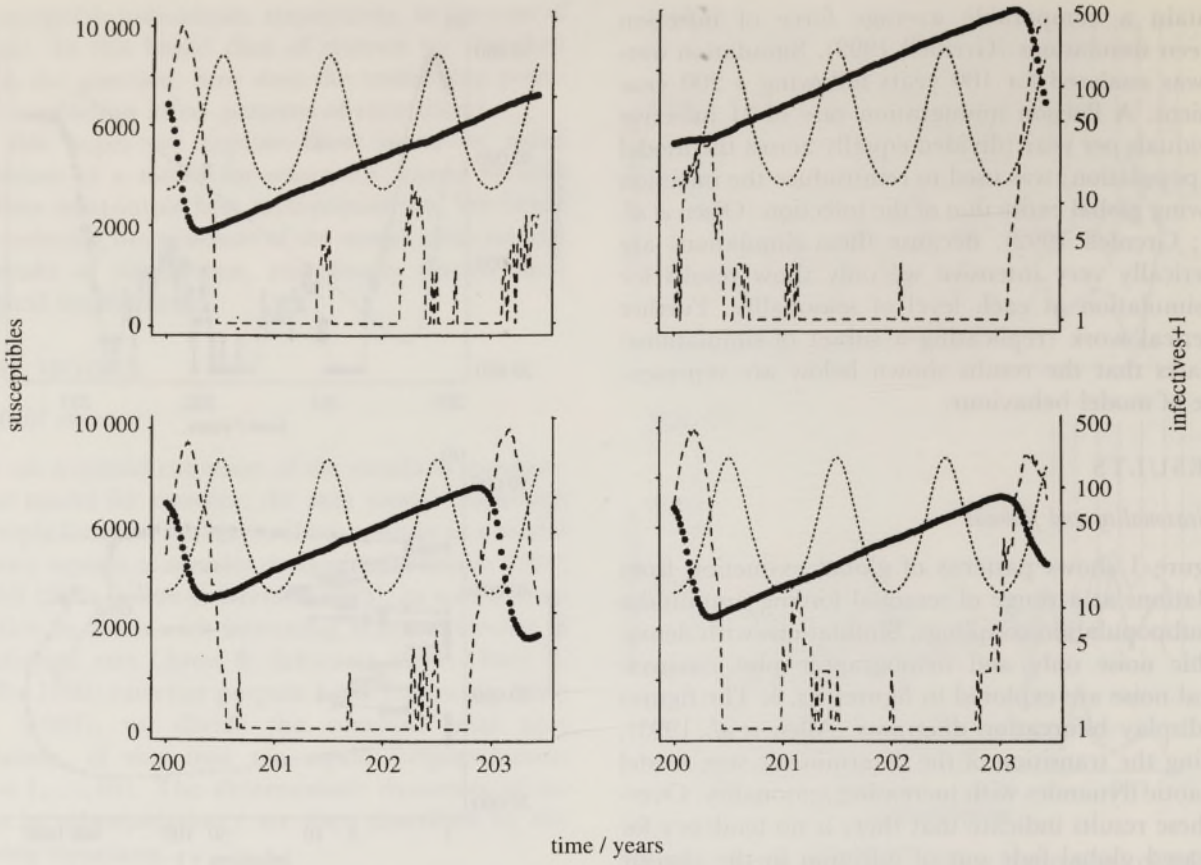

Figure 4. Time plots of susceptible (bold dots) and infective (broken line) densities for four of the ten subpopulations, corresponding to figure 3*a*. The periodic dotted curve is the critical local density of susceptibles for establishment of the infection, calculated from equation (2).

correlation of subpopulation for the case of demographic noise only (corresponding to figure 1*a*). In the simple deterministic, non-spatial SEIR model, increased seasonal forcing causes period doubling and eventually large amplitude chaos (see figure 1*a*). However, as shown in figure 2, increased seasonality in the spatial analogue also causes an increased correlation between subpopulations. Contrary to the result for the logistic map (Allen *et al.* 1993; Ruxton 1994), this increased correlation offsets any tendency for chaos-amplified noise to decrease overall population fade out. We stress that the absence of a negative association between chaotic dynamics and fade out is not specific to measles but is likely to be a generic property of forced predator–prey systems. Figure 2 also indicates that the slope of the approximately linear relation between correlation and seasonality increases with the degree of coupling of the metapopulation. Although this effect is partly a function of the slight increase in fadeout with coupling (see figure 1), it derives mainly from the correlation structure. Specifically, increased coupling raises the lower limit of correlation between subpopulations (which occurs at the lowest level of seasonality, see figure 2). For a given level of coupling, increased seasonality then magnifies correlation and hence fadeout.

(*b*) *Metapopulation persistence and host–parasite dynamics*

(i) *Dynamics of extinction.* Unlike the logistic map models of Allen *et al.* (1993) and Ruxton (1994), the above results arise from a population interaction between infective and susceptible hosts. The effects of this essentially predator–prey interaction on patterns of metapopulation persistence are explored in figures 3 and 4. Figure 3 begins with total susceptible (S) and infective (I) metapopulation trajectories from a section of simulation in the chaotic region ($b_1 = 0.33$), which shows significant degrees of fadeout of infection. The time series (see figure 3*a*) and associated S versus I phase plot indicate two major epidemics, separated by an infective trough in which the infection repeatedly becomes extinct and is reintroduced by the infective immigration rate. These results clearly illustrate the impact of the underlying population interaction on patterns of metapopulation extinction of infection. First (years 200 and 201) the initial large epidemic depletes the overall density of susceptibles and the infection disappears. Infection is then repeatedly reintroduced by immigration (years 201–202.5). However, although there are minor epidemics associated with the seasonal increase in infection rate (the latter illustrated by point size in figure 3), a major epidemic (year 203) can only occur when susceptible density has been increased sufficiently by births. The equivalent phase portrait (see figure 3*b*), which reflects the characteristic clockwise loop of predator–prey interactions, illustrates this buildup of susceptibles very clearly.

These results for the metapopulation aggregate could, in principle, conceal significant spatial detail in the dynamics. Figure 4 shows the infective and

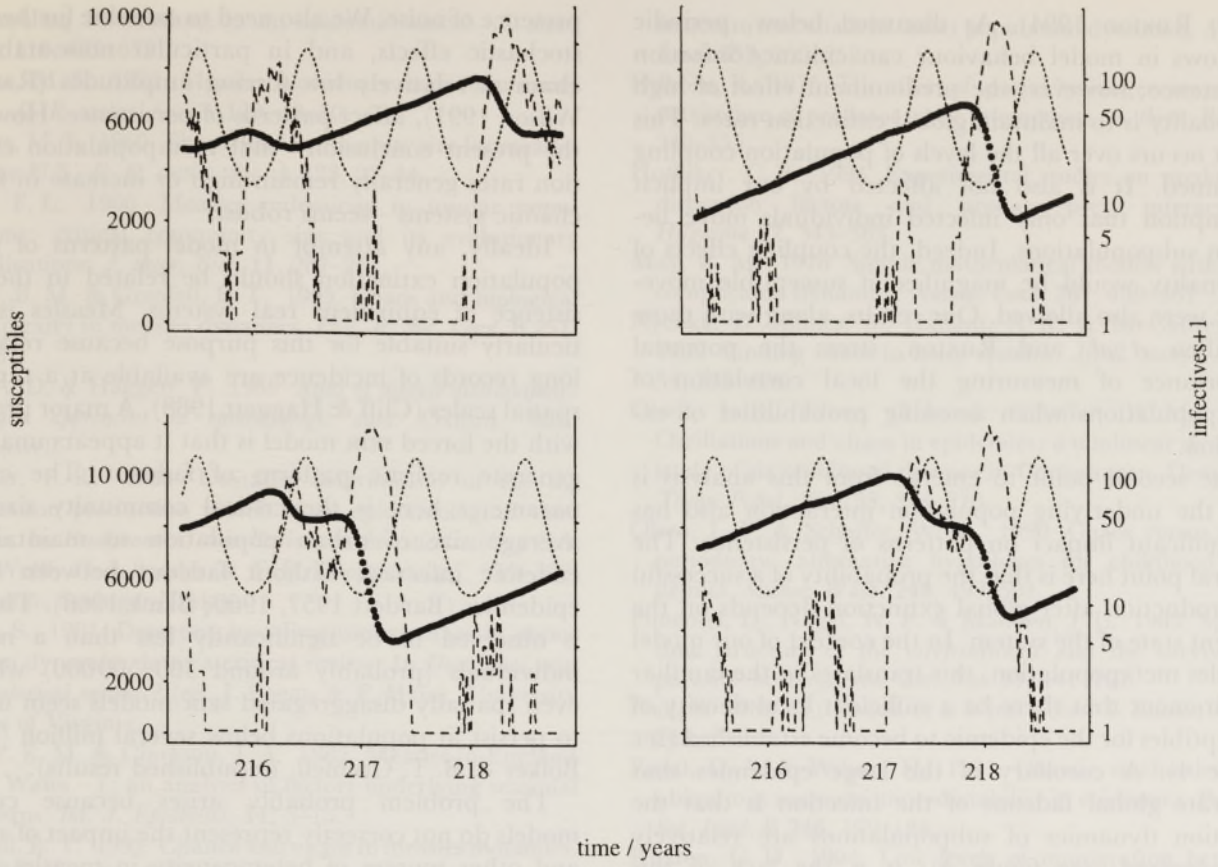

Figure 5. As figure 4, but for the simulation of figure 3*c*.

susceptible time series for individual subpopulations, corresponding with the aggregate results of figures 3*a*, *b*. Overall, the subpopulations are well correlated; the mean correlation of each with the rest of the aggregate is 0.873, with range 0.43 to 0.96, i.e. most of the susceptible series reflect the decline and subsequent approximately linear increase of the aggregate susceptibles (see figure 3*a*).

Finally, we can explore the timing of epidemics by calculating the critical local threshold density of susceptibles above which a reintroduced infection will become established. From the equilibrium of equations (1), it is routine to show that the effective reproductive ratio of infection is greater than unity, and that a reintroduced infection will therefore spread (Anderson & May 1991) above the susceptible threshold.

$$S_j \simeq \gamma/\{\beta(t)\,[1+(m-1)\nu]\}. \qquad (2)$$

Figure 4 displays this threshold; it is periodic, dropping seasonally as infection rates increase. According to simple theory, epidemics are more likely to establish when the local susceptible density is above this limit. Both the subpopulation series (figure 4) and, in particular, the aggregate data (see figure 3*a*) indicate that this is a good approximate criterion for the seasonal sequence of minor epidemics, as well as the synchronous accumulation of susceptibles before the major epidemic in year 203.

(ii) *Dynamics of metapopulation persistence.* For comparison with these results, figure 3 also shows a time series (see figure 3*c*) and phase plot (see figure 3*d*) from a section of the same simulation with no fadeouts. The metapopulation dynamics are dramatically different, reflecting an annual pattern of epidemics which is of much lower amplitude than the three-year cycle of figure 3*a*. The local dynamics (see figure 5) are even more distinct; the aggregate annual cycles are formed from an irregular and out-of-phase mixture of one-, two- and three-year epidemics at the local level. This local irregularity is reflected in the generally low correlation of susceptibles in each subpopulation with the rest of the aggregate (mean correlation 0.198, range −0.65 to 0.86) although there is considerable local fadeout, populations are sufficiently out of phase to offset global extinction.

In summary, the details of the population interaction (as well as the pattern of seasonality) have a strong influence on the timing of metapopulation extinction. These results also illustrate that high degrees of fadeout are associated with global synchronization of local susceptible populations, following large global epidemics.

4. DISCUSSION

This paper illustrates that the interaction between chaos and metapopulation persistence depends crucially on the origins of the former. By contrast with coupled discrete maps, simple models of seasonally forced predator–prey and host–parasite systems (such as measles) illustrate that strong seasonality tends to maintain or increase metapopulation extinction rates in chaotic systems by offsetting the ability of chaos to generate local differences in dynamics (Allen *et al.*

1993; Ruxton 1994). As discussed below, periodic windows in model behaviour can enhance infection persistence; however, the predominant effect of high seasonality is to maintain global extinction rates. This effect occurs over all the levels of population coupling examined. It is also not affected by our implicit assumption that only infected individuals move between subpopulations. Indeed, the coupling effects of seasonality would be magnified if susceptible movement were also allowed. Our results, along with those of Allen *et al.* and Ruxton, stress the potential importance of measuring the local correlation of metapopulations when assessing probabilities of extinction.

The second point to emerge from this analysis is that the underlying population interaction also has a significant impact on patterns of persistence. The general point here is that the probability of a successful reintroduction after global extinction depends on the current state of the system. In the context of our model measles metapopulation, this translates to the familiar requirement that there be a sufficient local density of susceptibles for the epidemic to become established (see figure 4). A corollary of the large epidemics that generate global fadeout of the infection is that the infection dynamics of subpopulations are relatively synchronized (see figure 4); it is the lack of this synchronization which prevents extinction (see figure 5). The latter effect is exactly that postulated by Allen *et al.* (1993) and Ruxton (1994) to explain the reduction in extinctions. Our results show that both periods of persistence and extinction are possible over a wide range of seasonal forcing amplitudes, given the complex intermittent dynamics of the SEIR model (Schwartz 1985; Bolker & Grenfell 1993). However, the synchronized major epidemic behaviour, with associated global fadeouts, is maintained or increased with increased seasonality.

As illustrated in figures 3–5, adding spatial heterogeneity to the forced SEIR model superimposes another level of complexity onto an already intricate dynamical picture. For example, point A in figure 1*a* (the level of fadeout for $b_1 = 0.32, v = 0.001$) indicates a lower extinction rate of infection than the points surrounding it (at $b_1 = 0.31, 0.33$). Extensive simulations of the deterministic model with random starting conditions indicates that the attractor for $b_1 = 0.32$ has a propensity for relatively low amplitude (low fadeout) biennial cycles, compared with $b_1 = 0.31$ and 0.33. However, in the spatial stochastic system, this manifests itself as a comparatively high frequency of annual metapopulation epidemics, with a significant component of out-of-phase biennial patterns in the subpopulations. These results reinforce the point (Sugihara *et al.* 1990) that the apparent effect of dynamic nonlinearities can depend crucially on the spatial scale on which they are observed. More work clearly needs to be done to clarify the nonlinear behaviour of forced spatial epidemic models. An important first step here has been made by Schwartz (1992), who analysed pairs of weakly coupled centres. However, much less work has been done to clarify spatial chaos in more complex forced systems in the presence of noise. We also need to examine further how stochastic effects, and in particular noise-stabilized chaos at relatively low forcing amplitudes (Rand & Wilson 1991), affect patterns of persistence. However, the present conclusion – that metapopulation extinction rates generally remain high or increase in forced chaotic systems – seems robust.

Ideally, any attempt to model patterns of metapopulation extinction should be related to the persistence of equivalent real systems. Measles is particularly suitable for this purpose because relatively long records of incidence are available at a range of spatial scales (Cliff & Haggett 1988). A major problem with the forced SEIR model is that it appears unable to generate realistic patterns of fadeout. The crucial parameter here is the critical community size, the average size of urban population to maintain an endemic infection without fadeout between major epidemics (Bartlett 1957, 1960; Black 1966). This size is observed to be significantly less than a million individuals (probably around 300–500000) whereas even spatially disaggregated SEIR models seem unable to persist at populations below several million (B. M. Bolker & B. T. Grenfell, unpublished results).

The problem probably arises because current models do not correctly represent the impact of spatial and other sources of heterogeneity in measles transmission. For example, one possible spatial refinement is to subdivide our metapopulation more finely. Preliminary analyses indicate that this can reduce the degree of global extinction of infection. However, it also tends to generate unrealistic annual cycles (analogous to those in figure 3*c*, *d*). Our model also implicitly neglects the effect of distance on mixing of subpopulations. High 'local' mixing could again act to promote persistence of the infection (Hassell *et al.* 1991). Preliminary work indicates that demographic noise and long range mixing in the stochastic SEIR system tends to destabilize low-amplitude, low-extinction patterns arising from local mixing.

Including other heterogeneities, for example, an age structure, mitigates these problems of fadeout somewhat (Bolker & Grenfell 1993). However, explaining fully the dynamics of metapopulation persistence in measles, along with morbilivirus infections of other mammals (Grenfell *et al.* 1992, 1994), remains a challenge for both epidemiologists and ecologists.

We thank the following for financial support: Isaac Newton Institute for Mathematical Science (B.T.G.), Royal Society and AFRC (A.K.) and Mellon Foundation (B.M.B.).

REFERENCES

Allen, J. C., Schaffer, W. M. & Rosko, D. 1993 Chaos reduces species extinction by amplifying local population noise. *Nature, Lond.* **364**, 229–232.

Anderson, R. M., Grenfell, B. T. & May, R. M. 1984 Oscillatory fluctuations in the incidence of infectious disease and the impact of vaccination: time series analysis. *J. Hyg., Camb.* **93**, 587–608.

Anderson, R. M. & May, R. M. 1991 *Infectious diseases of humans: dynamics and control.* Oxford University Press.

Aron, J. L. & Schwartz, I. B. 1984 Seasonality and period

– doubling bifurcations in an epidemic model. *J. theor. Biol.* **110**, 665–679.

Bartlett, M. S. 1957 Measles periodicity and community size. *Jl. R. statist. Soc.* A **120**, 48–70.

Bartlett, M. S. 1960 The critical community size for measles in the U.S. *Jl. R. statist. Soc.* A **123**, 37–44.

Black, F. L. 1966 Measles endemicity in insular populations: critical community size and its evolutionary implications. *J. theor. Biol.* **11**, 207–211.

Bolker, B. M. & Grenfell, B. T. 1993 Chaos and biological complexity in measles dynamics. *Proc. R. Soc. Lond.* B **251**, 75–81.

Cliff, A. D. & Haggett, P. 1988 *Atlas of disease distributions: analytic approaches to epidemiologic data.* Oxford: Basil Blackwell.

Drepper, F. R. 1988 Unstable determinism in the information production profile of an epidemiological time series. In *Ecodynamics: contributions to theoretical ecology* (ed. W. Wolff, C.-J. Soeder & F. R. Drepper), pp. 319–332. London: Springer-Verlag.

Ellner, S. 1991 Detecting low-dimensional chaos in population dynamics data: a critical review. In *Does chaos exist in ecological systems?* (ed. J. Logan & F. Hain). University Press of Virginia.

Fine, P. E. M. & Clarkson, J. A. 1982 Measles in England and Wales – I: an analysis of factors underlying seasonal patterns. *Int. J. Epidemiol.* **11**, 5–15.

Grenfell, B. T. 1992 Chance and chaos in measles dynamics. *Jl. R. statist. Soc.* B **54**, 383–398.

Grenfell, B. T. & Anderson, R. M. 1985 The estimation of age-related rates of infection from case notifications and serological data. *J. Hyg. Camb.* **95**, 419–436.

Grenfell, B. T., Lonergan, M. E. & Harwood, J. 1992 Quantitative investigations of the epidemiology of phocine distemper virus (PDV) in European common seal populations. *Sci. tot. Envir.* **115**, 15–28.

Grenfell, B. T., Kleczkowski, A., Ellner, S. & Bolker, B. M. 1994 Measles as a case study in nonlinear forecasting and chaos. *Phil. Trans. R. Soc. Lond.* A **348**, 515–530.

Hamer, W. H. 1906 Epidemic disease in England – the evidence of variability and of persistency of type. *Lancet* (i), 733–739.

Hanski, I., Turchin, P., Korpimaki, E. & Henttonen, H. 1993 Population oscillations of boreal rodents: regulation by mustelid predators leads to chaos. *Nature, Lond.* **364**, 232–235.

Hassell, M. P., Comins, H. N. & May, R. M. 1991 Spatial structure and chaos in insect population dynamics. *Nature, Lond.* **353**, 255–258.

Hilborn, R. 1975 The effect of spatial heterogeneity on the persistence of predator–prey interactions. *J. theor. Biol.* **8**, 346–355.

Huffaker, C. B. 1994 Experimental studies on predation: dispersion factors and predator–prey interactions. *Hilgardia* **27**, 343–383.

May, R. M. 1976 Simple mathematical models with very complicated dynamics. *Nature, Lond.* **261**, 459–467.

Nychka, D., Ellner, S., Gallant, A. R. & McCaffrey, D. 1992 Finding chaos in noisy systems. *Jl. R. statist. Soc.* B **54**, 399–426.

Olsen, L. F., Truty, G. L. & Schaffer, W. M. 1988 Oscillations and chaos in epidemics: a nonlinear dynamic study of six childhood diseases in Copenhagen, Denmark. *Theor. Popul. Biol.* **33**, 344–370.

Olsen, L. F. & Schaffer, W. M. 1990 Chaos versus noisy periodicity: alternative hypotheses for childhood epidemics. *Science, Wash.* **249**, 499–504.

Pimentel, D., Nagel, W. P. & Madden, J. L. 1963 Space–time structure of the environment and the survival of parasite–host systems. *Am. Nat.* **97**, 141–167.

Pool, R 1989 Is it chaos, or is it just noise? 1. *Science, Wash.* **243**, 25–28.

Rand, D. A. & Wilson, H. 1991 Chaotic stochasticity: a ubiquitous source of unpredictability in epidemics. *Proc. R. Soc. Lond.* B **246**, 179–184.

Ruxton, G. D. 1994 Low levels of immigration between chaotic populations can reduce system extinctions by inducing asynchronous regular cycles. *Proc. R. soc. Lond.* B **256**, 189–193.

Schenzle, D. 1984 An age-structured model of pre- and post-vaccination measles transmission. *IMA. J. math. appl. Med. Biol.* **1**, 169–191.

Schwartz, I. B. 1985 Multiple recurrent outbreaks and predictability in seasonally forced nonlinear epidemic models. *J. math. Biol.* **21**, 347–361.

Schwartz, I. B. 1992 Small amplitude, long period outbreaks in seasonally driven epidemics. *J. math. Biol.* **30**, 473–491.

Soper, M. A. 1929 The interpretation of periodicity in disease prevalence. *Jl. R. statist. Soc.* A **92**, 34–61.

Sugihara, G., Grenfell, B. T. & May, R. M. 1990 Distinguishing error from chaos in ecological time series. *Phil. Trans. R. Soc. Lond.* B **330**, 235–251.

Received 5 September 1994; accepted 10 October 1994